

MOUNTAIN-PLAINS CONSORTIUM

MPC 16-312 | S. Chen and L. Chen

Earthquake Fragility
Assessment of Curved and
Skewed Bridges in Mountain
West Region



A University Transportation Center sponsored by the U.S. Department of Transportation serving the Mountain-Plains Region. Consortium members:

Colorado State University
North Dakota State University
South Dakota State University

University of Colorado Denver
University of Denver
University of Utah

Utah State University
University of Wyoming

Earthquake Fragility Assessment of Curved and Skewed Bridges in Mountain West Region

by

Luke Chen

Suren Chen

Department of Civil and Environmental Engineering
Colorado State University
Fort Collins, CO 80523

September 2016

Acknowledgement

The funds for this study were provided by the United States Department of Transportation to the Mountain-Plains Consortium (MPC). The finite element models used in this study were modified from those developed by a former graduate student Thomas Wilson in a project funded by Colorado Department of Transportation.

Disclaimer

The contents of this report reflect the views of the authors, who are responsible for the facts and the accuracy of the information presented. This document is disseminated under the sponsorship of the Department of Transportation, University Transportation Centers Program, in the interest of information exchange. The U.S. Government assumes no liability for the contents or use thereof.

NDSU does not discriminate in its programs and activities on the basis of age, color, gender expression/identity, genetic information, marital status, national origin, participation in lawful off-campus activity, physical or mental disability, pregnancy, public assistance status, race, religion, sex, sexual orientation, spousal relationship to current employee, or veteran status, as applicable. Direct inquiries to Vice Provost for Title IX/ADA Coordinator, Old Main 201, NDSU Main Campus, 701-231-7708, [ndsu.eoaa.ndsu.edu](https://www.ndsu.edu/eoaa).

ABSTRACT

Reinforced concrete (RC) bridges with both skew and curvature are common in areas with complex terrains. Skewed and/or curved bridges were found in existing studies to exhibit more complicated seismic performance than straight bridges, however the related seismic risk studies are still rare. These bridges have irregular and complex geometric designs, and comprehensive seismic analysis is not always required. As a result, little knowledge about actual seismic risks for these bridges in low-to-moderate regions is available. To provide more insightful understanding of the seismic risks, analytical fragility studies were carried out on four typical bridge designs with different geometric configurations (i.e. straight, curved, skewed, skewed and curved) in the mountain west region of the United States. Results show curved and skewed geometries can considerably affect the bridge seismic fragility in a complex manner. Conducting a detailed seismic risk assessment of skewed and curved bridges is needed in low-to-moderate seismic regions.

TABLE OF CONTENTS

1. INTRODUCTION AND LITERATURE REVIEW	1
1.1 Background.....	1
1.1.1 BRIDGE SEISMIC HAZARD	1
1.2 Motivation of the Present Study	2
1.3 Organization of the Report	3
2. BRIDGE MODELING WITH SAP2000.....	4
2.1 Prototype Bridges	4
2.2 3-D finite element models.....	6
3. SENSITIVITY ANALYSIS AND EARTHQUAKE RECORDS	8
3.1 Uncertainties of Bridge Structures and Sensitivity Analysis.....	8
3.1.1 Compressive Concrete Strength.....	9
3.1.2 Steel Yield Strength	10
3.1.3 Damping Ratio	10
3.1.4 Superstructure Weight	10
3.2 Ground Motion Simulation for Fragility Analysis.....	10
3.2.1 Ground Motion from Database Record.....	10
3.2.2 Synthetic Ground Motion.....	11
4. ANALYTICAL FRAGILITY ANALYSIS.....	13
4.1 Theoretical Formulation	13
4.2 Limit States.....	15
4.2.1 Column Moment Curvature	15
4.2.2 Pier-Column Shear Strength	15
4.2.3 Abutment and Wing-Wall Deformation.....	16
4.3 Regression Analysis to Develop PSDM	16
4.4 Fragility Curve.....	20
4.5 Comparative Study of Critical Factors	21
5. CONCLUSION AND FUTURE WORKS	27
REFERENCES.....	28

LIST OF TABLES

Table 2.1	Geometric Configurations of Bridge Model	6
Table 3.1	Bridge Uncertainties Distribution	9
Table 3.2	Bridge Uncertainties Assignment Based on LHS	9
Table 3.3	Ground Motion Records from PEER	11
Table 3.4	Synthetic Ground Motions Generated for this Study	12
Table 4.1	Limit States Used in the Study with Mean Values and Correlation Factors	15
Table 4.2	Probabilistic Seismic Demand Parameter Regression of Straight Bridge Model	19

LIST OF FIGURES

Figure 2.1	The prototype 3D FEM bridge model and the variations	5
Figure 2.2	(a) Curved and skewed bridge dimension – radius 4500 ft. skew 300	5
Figure 2.3	Section modeling details	6
Figure 3.1	Sensitivities analysis result	8
Figure 4.1	Schematic diagram for component fragility curves construction	14
Figure 4.2	Column longitudinal curvatures PSDM for both Skewed and curved bridge	17
Figure 4.3	Column longitudinal curvatures PSDM for straight bridge	17
Figure 4.4	PSDM of column longitudinal shear strength for the curved and skewed bridge	18
Figure 4.5	PSDM of column transverse shear strength for the curved and skewed bridge	18
Figure 4.6	PSDM of abutment deformation	19
Figure 4.7	Component fragility curves	20
Figure 4.8	Column fragility curves of longitudinal moment curvature under light damage	22
Figure 4.9	Fragility median PGA of column curvature for different models under light damage	23
Figure 4.10	Skew and curvature influence on component fragilities under moderate damage state	23
Figure 4.11	Comparison of different geometric configurations under different damage states	24
Figure 4.12	Median PGA values comparison for abutment fragilities under different damage states	25
Figure 4.13	Median PGA comparison of skew and curvature influence on shear curves	26

1. INTRODUCTION AND LITERATURE REVIEW

1.1 Background

This Section encompasses necessary background information for the study. Topics covered include bridge seismic hazard, multiple hazard resistance, load interactions of traffic and bridges, and interactions of bridge seismic and scour.

1.1.1 BRIDGE SEISMIC HAZARD

The primary natural hazards being designed in major structural design codes in the United States are: earthquakes, floods, and high winds. Earthquakes are possibly the most difficult natural hazard to be designed for due to the lack of warning, rarity in frequency, and extreme consequences (FEMA 2004). Despite new advancements in the field of seismology, it is still difficult to predict the magnitude, location and time of occurrence for any particular earthquake. However, general characterization of the magnitudes and frequency of a region can be made based on geological setting and historical records. Some areas are more vulnerable to larger or less frequent earthquakes, while others may suffer from more frequent mild or moderate earthquakes. In structural design codes, seismic hazard maps provide information on the relative seismic exposure by assigning a hazard coefficient based on the probability of experiencing an earthquake, and its relative magnitude. This coefficient determines the necessary design requirements needed to be met through the code design approach.

The need for continued improvement on the resistance of bridges to earthquakes also is due to their unique importance in society as compared to other structures. Bridges are categorized as lifelines in inventories of the national infrastructure and assets. Critical bridges are necessary to help facilitate rescues, rebuilding, and other emergency services in the aftermath of a seismic event. Many studies have been conducted on assessing and improving the post-earthquake functionality of bridges. Part of this study, in line with these previous efforts, is to more realistically assess the safety and serviceability of a critical bridge by considering the interaction with other extreme loads, as well as normal service loads.

Bridges are key components of modern transportation systems and are typically regarded as lifeline infrastructures of a society. Functional bridges after a major seismic event not only provide effective evacuation path for residents, but also ensure connection of the seismic-affected areas for emergency response personnel to render prompt recovery and retrofiting efforts. In addition to many regular straight highway bridges around the world, horizontally curved and skewed bridges are often built to accommodate local site and terrain constraints with irregular geometric configurations, such as in the Mountain West region of the United States.

In most related researches, influences of bridge skew angle and curvature were studied separately on seismic performance. It was found that bridges with skew and those with curvature share some common vulnerabilities, such as being susceptible to deck unseating, tangential joint damage, pounding effects, and large in-plane displacements and rotations of the superstructure ([Saiidi and Orié 1992](#); [Maragakis, 1984](#); [Mwafy and Elnashi, 2007](#); [Wilson et al. 2014](#)). However, the seismic studies on bridges with combined curved and skewed geometric

configurations are rare. Recently, [Wilson et al. \(2014\)](#) studied the seismic performance of a suite of bridges located in the Mountain West region, including those with both curvature and skew. In their study, nonlinear time-history analysis was conducted on each bridge under a number of earthquake records scaled to the bridge site in Denver, CO. Since the Mountain West region traditionally is classified as a low-to-moderate seismic zone and requires no specific seismic design, such a study offered important insights on the global performance of these bridges subjected to seismic loads.

Fragility curve is a popular tool that converts sophisticated seismic assessment into a relation between conditional damage probability and ground motion intensity (e.g. [Xiao and Ma 1997](#), [Kowalsky and Priestley 2000](#) and [Ellingwood and Kinali 2009](#)). Its concept is not only widely adopted in academic research fields, but also as standardized methodology, such as HAZUS-MH by Federal Emergency Management Agency (FEMA) ([Vickery et al. 2006](#)). Although many fragility studies have been conducted on regular bridges, only a few exist on skewed bridges. Sullivan and Nielson (2010) conducted sensitivity study of bridges with a variety of skewed angles and compared component responses in longitudinal and transverse directions. [Zakeri et al. \(2014\)](#) investigated the impacts of skew on seismic performance of the integral abutments and suggested that the component fragilities are independent of the geometric configuration if shear keys are added. Most of the existing fragility studies for geometrically irregular bridges showed that their seismic behavior is usually more complex compared to regular ones, deserving specific investigations. This is especially true for those curved and skewed bridges in the low-to-moderate seismic regions where bridges were designed often without comprehensive seismic analysis, and many existing and new curved and skewed bridges shared the same design as the straight counterparts. As a result, impacts of the geometric configuration with both curvature and skew on the bridge seismic fragility still remain unknown to the community. In this study, fragility analysis was conducted as an extension of the existing study by Wilson et al. (2014) to disclose associated risks of component failures and the impacts from the curved and skewed geometric configurations. A typical 3-span straight RC bridge in Denver, CO, has been modified with different curved and skewed geometries to generate a series of bridge models. The 3-D finite element models (FEM) for these bridges, which consider various uncertainties, were built with SAP2000 to evaluate combined influences from bridge curvature and skew to seismic vulnerability. With both recorded and synthetic ground motions, nonlinear time history analyses of the bridge models were conducted considering uncertainties associated with ground motions and structural properties. Component fragility curves for different bridge models were developed with the appropriately-defined limit states, followed by the comparative study about the influences from different geometric configurations. Results show high probability of pier-column damage and stacking effects on individual columns, which underscore the significance of the seismic risk assessment for skewed and curved bridges.

1.2 Motivation of the Present Study

The purposes of this study are to: (1) develop a general analytical methodology to study multiple service and extreme loads for short- and medium-span bridges, and (2) conduct numerical performance analysis of a typical bridge in a mountainous region subjected to seismic and other extreme and service loads, including scour and stochastic traffic. This was achieved through formulation of a detailed FEM-based modeling of a typical concrete multi-span bridge in

Colorado, and realistic modeling and quantification of traffic service loads and the rational consideration of the associated dynamic interactions with the bridge. Time-domain nonlinear analysis was conducted to evaluate the performance of the bridge under combined dynamic loads. The objectives were broken down into the following tasks:

First, the detailed FEM model of a typical medium-span pre-stressed concrete bridge in Colorado was developed with SAP 2000. Second, the stochastic traffic flow on the bridge was simulated with advanced traffic flow simulation tools. The dynamic time histories of moving wheel axle loads were quantified considering dynamic interactions. Third, the time histories of moving vehicles with interactions effects were applied on corresponding nodes of the FEM model to simulate dynamic traffic stochastic loads. Fourth, a collection of different scenarios of combined extreme and service loads, such as seismic, traffic and scour were studied to assess bridge performance. FEM models of the bridges included detailed superstructures, which provided more detailed performance information in order to include dynamic loads from the moving traffic. In addition, the following study also attempted to shed light on and quantify the effects of pier elongation from scour events in combination with seismic performance of typical highway bridges being modeled.

1.3 Organization of the Report

The report is composed of five sections:

Section 1 introduces pertinent background information and literature review results related to the present study.

Section 2 includes detailed information of FEM modeling results with SAP 2000 for different bridges is presented.

Section 3 includes reports for sensitivity analysis and the selected earthquake records.

Section 4 details the development of analytical fragility curves for the representative curved and skewed bridges. For comparison purposes, fragility curves of those straight counterparts also are developed and some comparative studies made.

The report concludes with Section 5, which offers a summary of the findings and some conclusions that can be drawn from the previous sections.

2. BRIDGE MODELING WITH SAP2000

The following Section describes the modeling process of a typical concrete bridge located in Colorado. The commercial software SAP2000 version 15.0.1, produced by Computers & Structures Inc., was used to conduct the bridge modeling and seismic analysis. The finite element models used in this Section were modified from those developed by former graduate student Thomas Wilson ([Wilson et al. 2014](#)).

2.1 Prototype Bridges

A 3-span straight highway bridge (D-17-DJ) on I-25, located in Denver, CO, was selected as the prototype bridge (Figure 2.1a) to represent local typical concrete girder bridges in the Mountain West region. The Colorado Department of Transportation assisted on selecting the prototype bridge, for which the geometric configurations, material and design details are common for its kind in the area. The prototype bridge consists of two identical side spans of 22.1 m each and a middle span of 29.5 m. The bridge is composed of 205 mm deep concrete slab deck supported by eight parallel pre-stressed concrete I-girders with 1.73 m depth and the integral connection was adopted to link the bridge deck and the abutment (Figure 2.1a).

To study curved and skewed bridges with realistic designs, some geometric variations from the straight prototype bridge were made based on a discussion with and guidance from the Colorado Department of Transportation ([Wilson et al. 2014](#)). The ranges of skew and curvature are representative of the actual ones adopted in the region. For low-to-moderate seismic region, curved and/or skewed bridges often adopt the same designs as the straight counterparts when the curvature and/or skew are moderate. Therefore, the design details for these bridges with geometric variations are the same as those for the prototype bridge. Such an arrangement has two advantages: (1) same design detail as the straight counterpart is common for curved and skewed bridge in the region, yet without comprehensive evaluation in terms of seismic performance and risk; (2) same design of these bridge models allows for better investigations on the effects from geometric configurations by excluding other possible influences. In the study conducted by [Wilson et al. \(2014\)](#), numerical investigations were made on seven bridge models with different curved and skewed configurations, as well as on the straight prototype bridge in terms of seismic performance following the [AASHTO LRFD design guideline \(AASHTO 2013\)](#). A baseline bridge model (Figure 2.1 (b, c)) was first constructed based on the actual prototype straight bridge as shown in Figure 2.1(a). As illustrated in Table 1, three representative bridge models with different curvature and skew configurations are modified from the baseline bridge model (i.e. curved only, skewed only and both skewed and curved). The FEM analytical model of the curved and skewed bridge is shown in Figure 2.1 (d, e). In the following sections, detailed fragility analyses were conducted for the four bridge models as listed in Table 2.1.

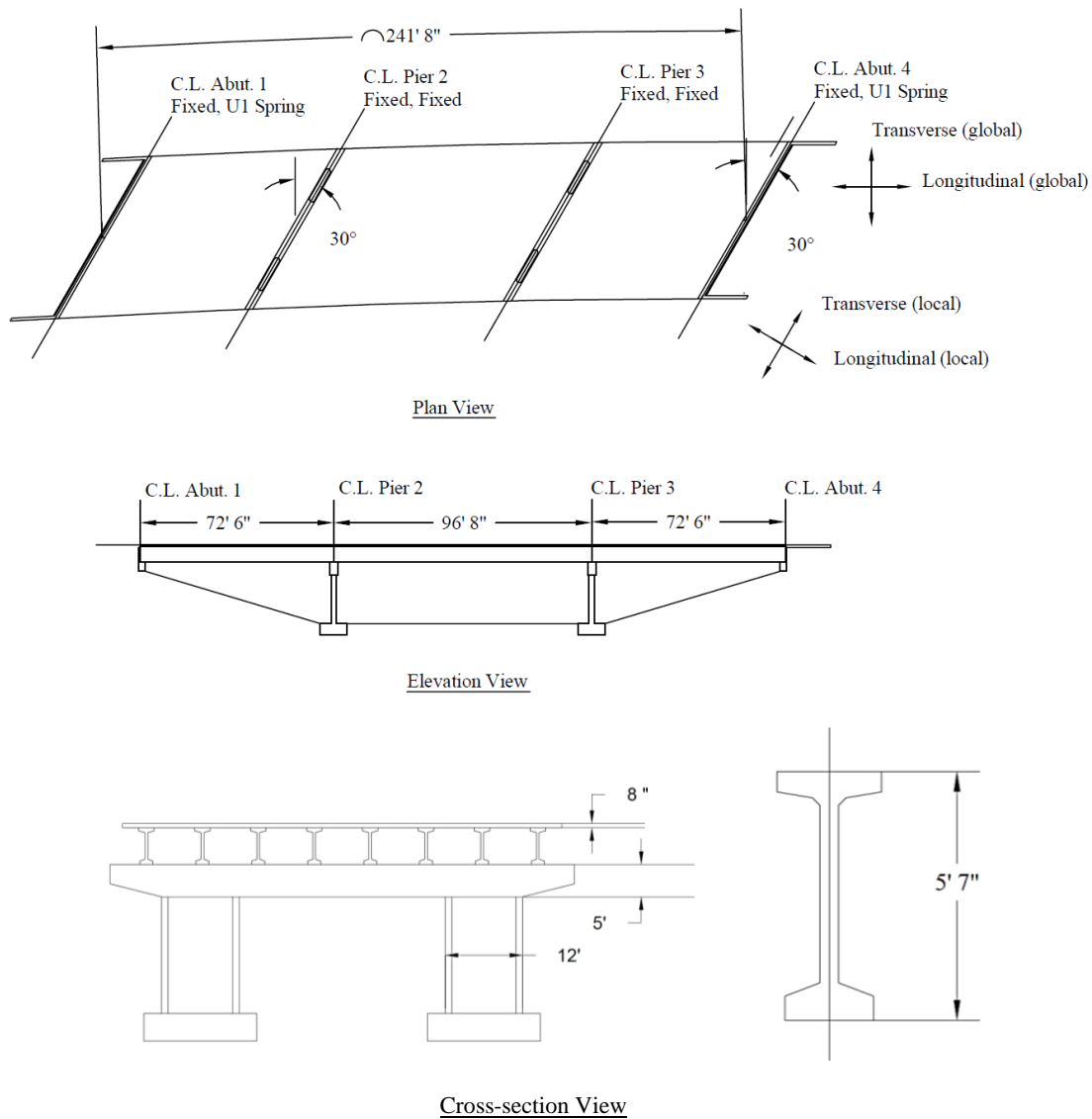
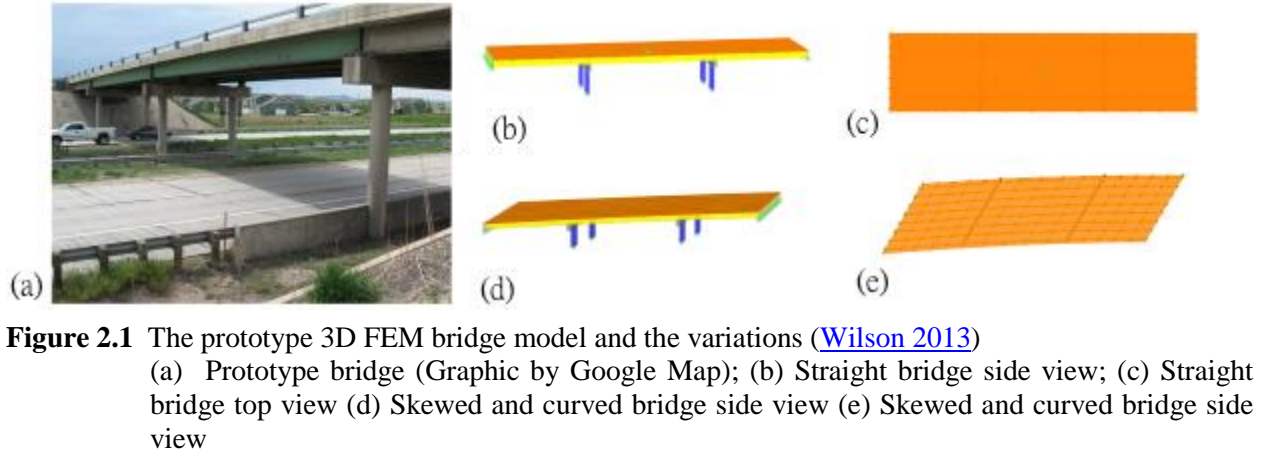


Table 2.1 Geometric Configurations of Bridge Model

Bridge Type	Skew (degrees)	Curvature Radius (ft)	Super Elevation (degrees)
Straight*	0	0	0
Skewed only	30	0	0
Curved only	0	3000	6
Skewed and Curved	30	3000	6

Note: *Baseline model

2.2 3-D finite element models

3-D FEM numerical models were developed with SAP2000 (CSI 2011) for the four bridge models listed in Table 1 to investigate the influence of skew and curvature on the seismic performance and risks. Figure 2 shows modeling details of the bridge components including columns, integral abutments, bent caps, and girders.

As shown in Figure 2.3, the four semi-ellipse columns are labeled as column A-D, which are modeled as beam elements for both columns and pier caps. The bottom of the bridge pier is fixed in the soil in all directions. To simulate post-yield behavior due to seismic loading, P-M2-M3 (coupled axial and biaxial-bending) plastic hinges were placed at both column ends with a relative distance suggested by the Washington State Department of Transportation Design Manual (WSDOT, 2011) because plastic deformation is localized in a small “plastic hinge zone” for RC flexural members. Gaps between each span were simply supported by concrete bent cap rigidly connected with two RC columns on each side.

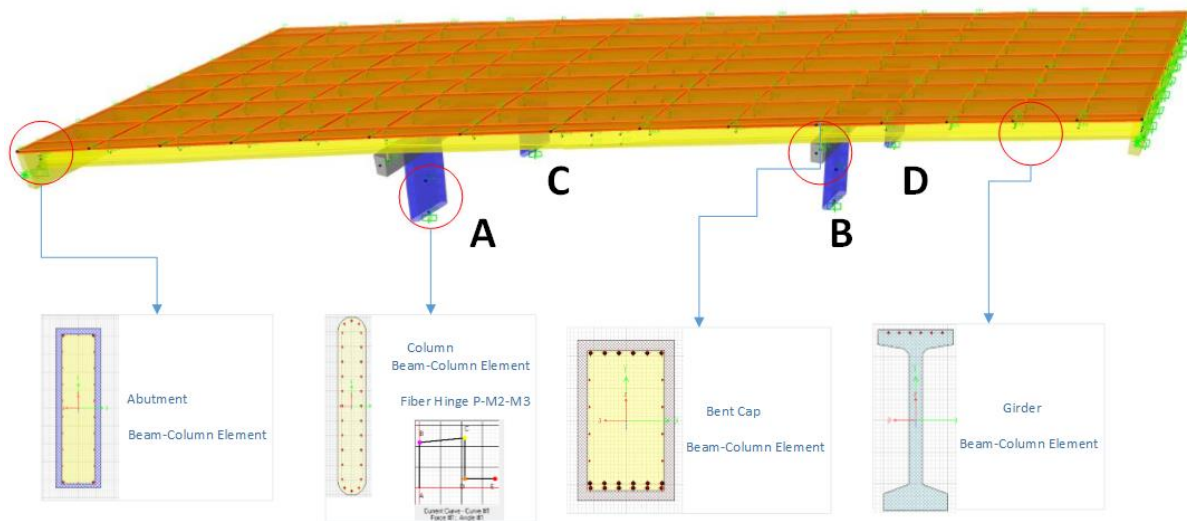


Figure 2.3 Section Modeling Details

The integral abutments of the bridges were also modeled as beam elements with rigid connections to the end of the girders. Pile foundations of the abutments in all directions were fixed except for the longitudinal direction. Multi-linear compressive spring elements were applied in this direction based on the California Department of Transportation (Caltrans) design procedures for backing soil behind an integral abutment ([Caltrans, 2006](#)). Plastic hinges with a lumped plasticity model were implemented at the top and bottom of the pier-columns to account for the inelastic column behavior of the substructure.

In most of the bridge fragility curve analyses, superstructures were modeled with simplified elements or lumped as concentrate mass attached to the substructure. To capture the geometric horizontal curvature characteristics in a better way, bridge decks were modeled as thin shell elements with 4 x 4 meshing. The eight girders were modeled as frame elements, which were connected with the bridge deck by use of fully constrained rigid links.

3. SENSITIVITY ANALYSIS AND EARTHQUAKE RECORDS

This section introduces the earthquake records used in the time-history analyses. Sensitivity analysis results also were reported in preparation for the following fragility analyses.

3.1 Uncertainties of Bridge Structures and Sensitivity Analysis

One major difference between the analytical fragility curve method and some other risk assessment methodologies is that the analytical fragility curve method uses a limited number of simulations instead of time-consuming Monte Carlo simulations. To complement this inherent statistical issue with limited samples, major uncertainties need to be considered. Most uncertainties associated with structures can be classified into two categories: epistemic and aleatory uncertainties. The former generally originates from model assumptions, simplified variables in formulas or lack of knowledge, which require statistical uncertainties being incorporated into the numerical model. The later one is attributed to inherent randomness in the seismic demand and capacity models, which means that the aleatory uncertainties should be considered when input ground motions or structural capacity models are selected.

Before incorporating structural uncertainties into the FEM models, an extensive sensitivity analysis was conducted to evaluate which variables are more critical in terms of considering uncertainties during the fragility curve development process. The sensitivity analysis was conducted under the excitation of the Whittier Narrows-01 earthquake (PGA=0.2g). The results show that concrete strength, steel yield strength, damping ratio, and superstructure weight significantly affect the bridge seismic performance and should be included into the models (Figure 3.1).

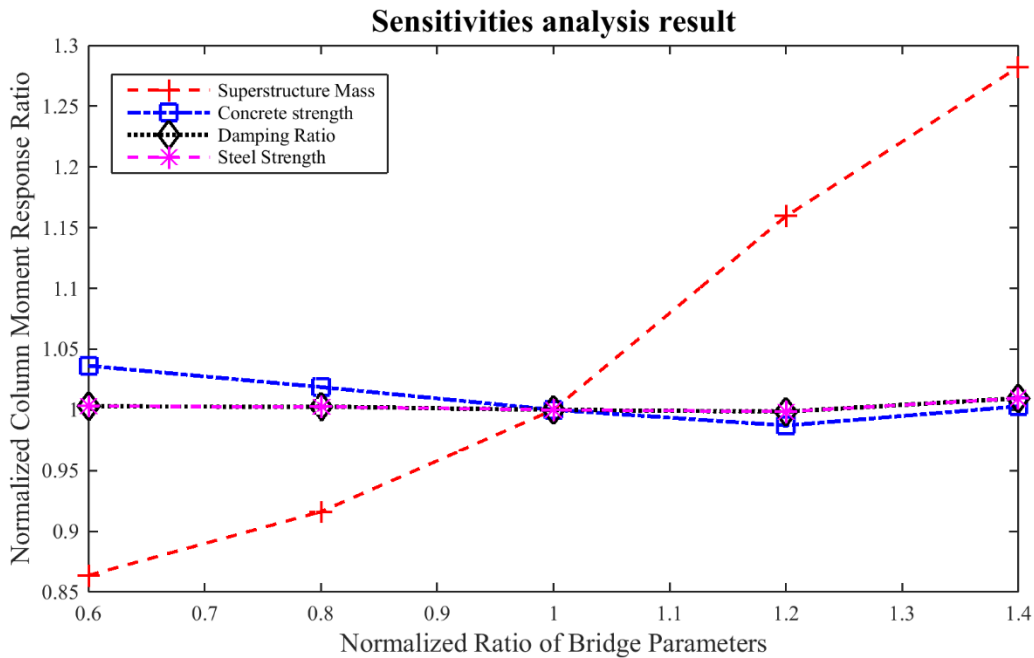


Figure 3.1 Sensitivities Analysis Result

In the absence of site-specific data, the uncertainty distributions of variables in this study were decided primarily based on a comprehensive literature review of similar variables in existing studies. Based on the site-specific conditions, several assumptions and modifications were made to accommodate specific bridge conditions. The uncertainty results are summarized in Table 3.1. The selected parameters based on the sensitivity analysis were then assigned to the models using Latin Hypercube sampling (LHS) approach (Neves et al., 2006). The sampling method was used to ensure variables allocated to model parameters based on particular probability distributions within a small number of samples, will eventually lower the epistemic uncertainties. After applying the LHS, variables were formed into a matrix, of which each row represents one FEM model with uncertainties (Table 3.2). In this study, eight models were generated for different geometric configurations, each of which was paired with 12 ground motions, generating 96 data points in total.

Table 3.1 Bridge Uncertainties Distribution

Bridge Parameter	Type of Distribution	Mean	Deviation	Units	Reference
Compressive Concrete Strength	Normal	35.8	5.376	Mpa	MacGregor et al. (1997)
Steel Yield Strength	Log-normal	463.3	37.07	Mpa	Ellingwood & Hwang (1985)
Damping Ratio	normal	0.045	0.00125		Fang et al.(1999)
Superstructure Weight	Uniform	0.9–1.1	0.0577		Nielson (2005)

Table 3.2 Bridge Uncertainties Assignment Based on LHS

	Density	f'c (kip)	Fy (kip)	Damping ratio
1	0.151436	794.3853	9555.788	0.064486
2	0.14665	665.9185	9799.357	0.051163
3	0.16435	777.6843	10388.54	0.044602
4	0.139488	735.7493	8559.162	0.039779
5	0.145969	835.3762	10940.39	0.035814
6	0.161118	758.4693	9305.725	0.025715
7	0.136277	725.8093	9013.831	0.046521
8	0.156359	708.7064	10062.69	0.056484

Note: f'c = Compressive Concrete Strength; Fy = Steel Yield Strength

3.1.1 Compressive Concrete Strength

Generally, the compressive concrete strength of bridges follows normal distributions, but its mean value can vary considerably over different regions in the United States. For example, eastern states such as New York, use 20.7 Mpa in their standard design, which results in the mean value of 27.2 MPa and a standard deviation of 4.24 MPa (Pan et al. 2007). However in Central and Southeastern United States (CSUS), concrete strength typically has the mean value of 33.5 MPa and standard deviation of 4.3 MPa (Nielson 2005). In this study, it was assumed

that the mean and standard deviation of the concrete strength were similar to those obtained from the 5-ksi class experimental data ([MacGregor et al. 1997](#)), which are 35.8Mpa and 5.376Mpa, respectively.

3.1.2 Steel Yield Strength

For composite material like concrete, the specific failure mode (e.g. shear failure or flexure failure) for RC columns is usually dependent on individual components of the composite material. Thus, the uncertainty characteristics of reinforced steel and concrete were considered separately in this study. According to the findings in the statistical study by [Ellingwood and Hwang \(1985\)](#), the strength characteristics of the reinforced bar are adopted to represent the steel strength uncertainty in this study. The steel strength follows lognormal distribution, with mean and standard deviation for steel strength being 463.3Mpa and 37.07Mpa, respectively.

3.1.3 Damping Ratio

The prototype bridge used in this study falls into the category of Multi-Span Continuous Concrete Girder (MSCCG) Bridges based on the definitions summarized in Nielson's study ([Nielson, 2005](#)). The uncertain distribution of the damping ratio applied in this study was based on the MSCCG data from the study by [Nielson and DesRoches \(2007\)](#). The mean and standard deviation of the damping ratio are 0.045 and 0.00125 respectively with normal distributions.

3.1.4 Superstructure Weight

Although the bridge superstructure typically has less direct effect from seismic ground motions compared to substructure and thus tends to remain linear behavior, its weight could still have considerable effects on the seismic performance due to horizontal curvature and asymmetric layouts. Following the findings by [Nielson \(2005\)](#), the uncertainty of superstructure weight is attributable to the material density of the bridge deck, which is assumed to have a uniform distribution for a ratio between 0.9 and 1.1.

3.2 Ground Motion Simulation for Fragility Analysis

Ground motions used in this study are a set of 96 earthquake records consisting of 48 real and 48 synthetic ground motions as described in the following sections. To study impacts of skew and curvature on bridge seismic performance, an input ground motion combination of 100% intensity in longitudinal direction and 40% in transverse direction was found to control the time history analysis ([Wilson et al. 2014](#)). The same ground combination is adopted in the following study.

3.2.1 Ground Motion from Database Record

Local seismic characteristics were considered during the selection from the Pacific Earthquake Engineering Research Center (PEER) ground motion database to properly reflect the seismic geographic features of Colorado. Earthquake magnitude with a range of 4.5 to 8.5 Richter magnitude is another indicator of seismic intensity, and is an indirect parameter for synthetic ground motion simulation introduced later in this study. Joyner-Boore distance (R_{jb}) for a

particular ground motion is the distance typically between 20 km to 100 km according to the study of the fault lines distribution in Colorado by [Matthews \(2003\)](#). Shear wave velocity (V_{s30}) is related to soil condition, which is the default D class soil with a range from 600 to 1200 ft/s according to the AASHTO LRFD specification ([AASHTO 2013](#)). Table 3.3 shows a typical suit of ground motion records used in this study.

Table 3.3 Ground Motion Records from PEER

Event	Year	Station	Longitudinal PGA (g)	Transverse PGA(g)
Morgan Hill	1984	SF Intern. Airport	0.04783	0.04781
Chalfant Valley-01	1986	Bishop - LADWP South St	0.12943	0.09441
Santa Barbara	1987	UCSB Goleta	0.34022	0.34022
Northridge	1994	5360 Saturn St., Los Angeles	0.42029	0.42029
Imperial Valley-06	1979	Delta	0.23776	0.35112
San Fernando	1971	LA – Hollywood Stor FF	0.20988	0.17418

3.2.2 Synthetic Ground Motion

Reliable Probability Seismic Demand Model (PSDM) requires representative ground motion inputs for time-history analysis to reduce aleatory uncertainties. In most of the interplate regions such as California, ground motions can be selected from the database including PEER or U.S. Geological Survey (USGS) covering low to high seismic intensities. The Mountain West region has a lack of strong ground motion records due to the intraplate geological characteristics, and therefore synthetic ground motions are widely applied in fragility curve studies of the areas without sufficient seismic records ([Choi 2002](#); [Nielson and DesRoches 2007](#); [Padgett and DesRoches 2007](#)). To incorporate good coverage of different intensities, synthetic ground motions generated for this study followed Nielson's work (2005) and modification developed by Baker and Cornell (2005). The generating procedure of synthetic ground motions is briefly introduced here: (1) Synthetic accelerograms were generated based on the determined parameters listed in section 5.1 and corrected in frequency domain. (2) Accelerograms were then adjusted to the site-specific target response spectrum according to the USGS map. (3) Every single synthetic ground motion was then used as a "seed" ground motion to generate orthogonal ground motions using correlation factors ([Baker and Cornell 2005](#)). Table 3.4 shows selected synthetic ground motions generated in this study.

Table 3.4 Synthetic Ground Motions Generated for this Study

Magnitude	Rjb (km)	Longitudinal PGA (g)	Transverse PGA(g)
6.0	60	0.57925	0.42831
6.5	60	0.64219	0.47302
7.0	60	0.51839	0.36556
6.0	40	0.58859	0.44692
6.5	40	0.70115	0.46789
7.0	40	0.81668	0.6134

ANALYTICAL FRAGILITY ANALYSIS

4.1 Theoretical Formulation

The following Section presents results of developing fragility curves. The first step in generating fragility curves was to establish a probability seismic demand model (PSDM). According to the study by [Baker and Cornell \(2006\)](#), the median of structural demand S_d can be statistically described as exponential distribution:

$$S_d = a * PGA^b \quad (4.1a)$$

or

$$\ln(S_d) = \ln(a) + b * \ln(PGA) \quad (4.1b)$$

where coefficients “a” and “b” can be determined by the regression analysis of data points obtained from time history analysis.

Based on Eqs. (4.1a-b), the cumulative conditional probability distribution of seismic demand exceeding a certain level of structural capacity C under the corresponding seismic intensity can be written once the standard deviation $\beta_{D|IM}$ is estimated:

$$P[D \geq C | IM] = 1 - \Phi\left(\frac{\ln(d) - \ln(aIM^b)}{\beta_{D|IM}}\right) \quad (4.2)$$

where $P[D \geq C | IM]$ = the conditional probability that the seismic demand of structure (D) is greater than structural capacity (C) under specific seismic intensity (IM). $\Phi(\cdot)$ = the standard normal cumulative distribution function. S_d = median value of seismic demand of the pre-defined limit state.

With the assumption that structural capacities and seismic demand both have lognormal distributions, the concept of demand/capacity ratio was introduced into Eq. (4.2) ([Nielson 2005](#)):

$$P[D \geq C | IM] = \Phi\left(\frac{\ln(S_d/S_c)}{\sqrt{\beta_{D|IM}^2 + \beta_c^2}}\right) \quad (4.3)$$

where S_c = median of the estimated capacity of the pre-defined limit state; β_c = standard deviation of the estimated capacity; $\beta_{D|IM}$ = seismic demand standard deviation under specific seismic intensity IM.

The key steps of to developing fragility curves are shown in the flowchart as shown in Figure 4.1 and summarized as follows:

1. Build 3-D FEM models for each bridge as listed in Table 1, including the straight bridge and the curved and skewed variations. Based on the sensitivity analysis, finalize uncertainties considered in the study and apply those variables with uncertainties to the developed models.
2. Select representative ground motions with intensities distributed from low to high based on the site characteristics. If the ground motion from the database record is lacking, synthetic ground motions are generated for appropriate intensity coverage.
3. Perform nonlinear time history analysis on the FEM bridge models with uncertainties considered, subjected to the representative ground motions. Obtain component seismic demands and apply regression analysis to obtain the coefficients “a” and “b” in Eq. (4.1b).
4. Define appropriate structural limit states from literature, specifications and survey.
5. Calculate analytical fragility curve following Eq. (4.3).

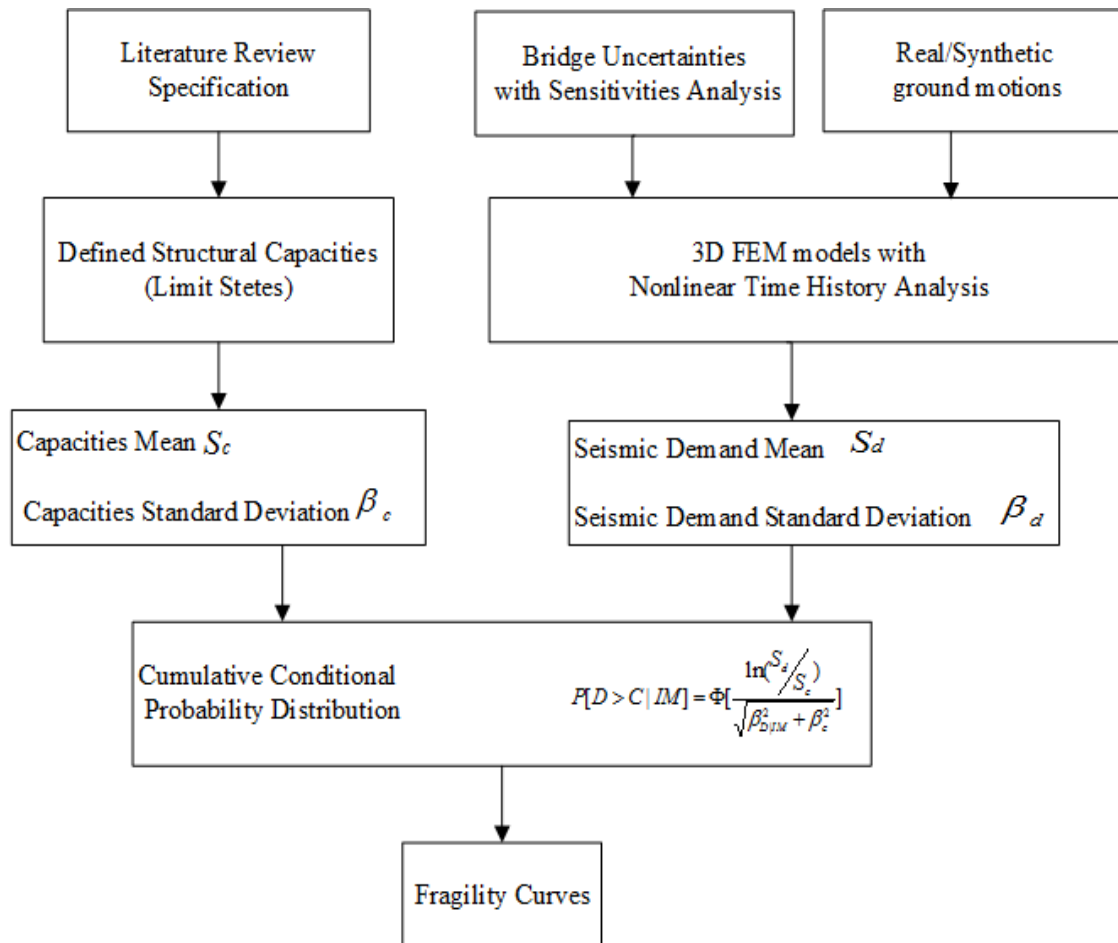


Figure 4.1 Schematic diagram for component fragility curves construction

4.2 Limit States

Structural capacities discussed in the previous section are defined by limit states (or damage states), which determine structural quantitative seismic demands causing damage to bridge components. In general, limit states can be determined through a physics-based (e.g. experimental) approach, descriptive (e.g. expert survey) approach ([Padgett and DesRoches 2007](#)) or Bayesian approach ([Nielson, 2005](#)). The descriptive criteria of limit states were first defined in [HAZUS 97 \(FEMA, 1997\)](#), which were followed in later studies in terms of limit state definitions. In this study, limit states were decided and based on literature review of the related studies. Those selected are listed in Table 4.1, with details illustrated as follows:

Table 4.1 Limit States Used in the Study with Mean Values and Correlation Factors

Component	Slight		Moderate		Extensive		Complete	
	S_c	β_c	S_c	β_c	S_c	β_c	S_c	β_c
Col-Long	0.0024515	0.59	0.0039908	0.51	0.0066893	0.64	0.009958	0.65
Col-Trans	0.0003359	0.59	0.0005467	0.51	0.0009164	0.64	0.0013642	0.65
Shr-Long (Kips)	N/A		N/A		N/A		731.59	N/A
Shr-Trans (Kips)	N/A		N/A		N/A		630.85	N/A
Abut-p (ft)	0.1213911	0.25	0.2427822	0.25	0.8497375	0.46	2.4278215	0.46
Abut-a (ft)	0.0593832	0.25	0.1190945	0.25	0.3569554	0.46	0.7139108	0.46
Wing (ft)	0.1213911	0.25	0.2427822	0.25	0.8497375	0.46	2.4278215	0.46

Note: S_c = Median values of component limit states; β_c = dispersions of component limit states; Col-Long = column longitudinal moment curvature; Col-Trans = column transverse moment curvature; Shr-Long = Pier-Column Longitudinal shear strength; Shr-Trans = Pier-Column Transverse shear strength; Abut-a = abutment active deformation; Abut-p = abutment passive deformation; Wing = wing wall deformation

4.2.1 Column Moment Curvature

Bridge columns are one of the critical components to seismic response, and can result in different failure modes. In most fragility curve studies, flexural damage to bridge column generally is quantified based on the drift ratio ([Shinozuka et al. 2002](#), [Mackie and Stojadinović 2007](#), [Zhang and Huo 2009](#)) or ductility ([Nielson and DesRoches 2007](#); [Padgett and DesRoches 2008](#)). For fragility curves in this study, curvature ductility was determined as the limit state following the survey conducted by [Padgett and DesRoches \(2007\)](#) based on expert opinions. It was adopted that the column ductility under light, moderate, extensive and complete damage states with the mean values of 1.29, 2.1, 3.52 and 5.24, and with the corresponding parameter β_c of 0.59, 0.51, 0.64 and 0.65, respectively.

4.2.2 Pier-Column Shear Strength

Shear force on the bridge pier-column component is also a critical demand and could easily exceed its capacity during a seismic event. Because shear failure is a type of brittle failure and hard to be assessed with different serviceability conditions, only the complete damage state for shear strength in both directions is considered based on its damage model. The shear damage

model of the total shear V_{total} considers the column concrete shear strength V_c , steel shear strength V_s and axial shear strength V_p (Priestley et al., 1996).

$$V_{total} = V_c + V_s + V_p \quad (4.4)$$

where

$$V_c = k\sqrt{f_c} A_e \cong 0.232\sqrt{f_c} A_g \quad (4.5a)$$

$$V_s = \frac{A_{sw} f_y D'}{s} \cot\theta = \frac{A_{sw} f_y D'}{s} \cot 30^\circ \quad (4.5b)$$

$$V_p = P \tan \alpha = \frac{D-c}{L} P \quad (4.5c)$$

k = constant based on member displacement ductility level (0.29 if using MPa unit); f_c' = concrete compressive strength; A_g =section gross area= $0.8 A_e$; A_{sw} = area of rebar; s =rebar spacing; L =rebar spacing; f_y = steel yield strength; θ = inclination to column axis (suggest as 30° based on plasticity theory); D =section diameter; P = axial force; c = compression zone depth; D' =rebar diameter; α = inclination to column axis.

4.2.3 Abutment and Wing-Wall Deformation

Abutment is another critical component for bridge seismic design, which has been often investigated in fragility studies (e.g. [Kwon and Elnashai 2007](#); [Billah et al. 2013](#)). Deformation due to seismic ground motions not only causes failure to the back wall, but also enhances particular behaviors such as pounding effect when skew is considered ([Zakeri et al. 2014](#)). According to the study by [Choi \(2002\)](#), passive deformation limit states of integral abutment are defined as fractions of the maximum deformation capacity of the back fill soil (y_{max}) such as $0.005 y_{max}$, $0.01 y_{max}$, $0.35 y_{max}$ and y_{max} for light, moderate, extensive and complete damage, respectively. In this study, y_{max} is assumed to be 2.42 ft following the study by [Sucuoğlu and Erberik \(2004\)](#).

4.3 Regression Analysis to Develop PSDM

The time history seismic analysis results of the selected structural components were represented as data points in the response-seismic intensity plots for nonlinear univariable regression analysis. According to observation in the previous studies, most bridge models experience stacking effect on different columns, causing different seismic behavior on the interior and exterior columns ([Wilson et al. 2014](#)). Therefore, regression analysis results for different columns were discussed individually.

With the assumption of lognormal distributions, the PSDM results of the longitudinal curvature for the skewed and curved bridge show considerable differences among different columns (Figure 4.2). For comparison purposes, the longitudinal curvature PSDM results for the straight bridge are shown in Figure 4.3. It is apparent that the PSDM results for the skewed and curved bridge are more scattered than those for the straight bridge. In the following fragility curve development, differences among regression lines of different columns also could affect the accumulation of probability distribution.

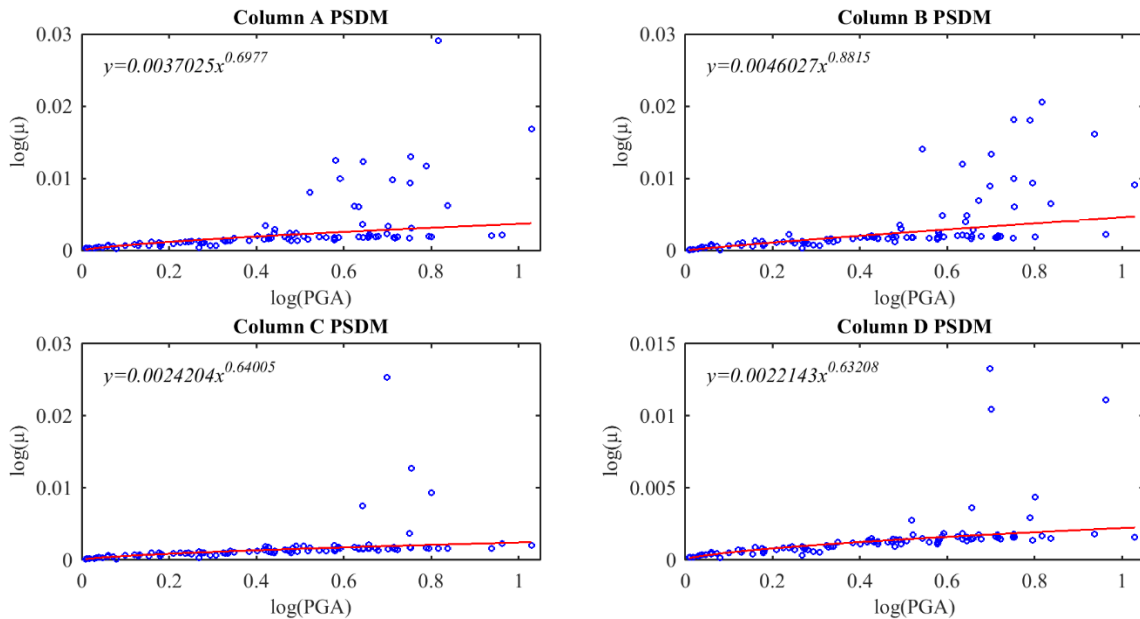


Figure 4.2 Column longitudinal curvatures PSDM for both Skewed and curved bridge
 Note: μ =component seismic demand

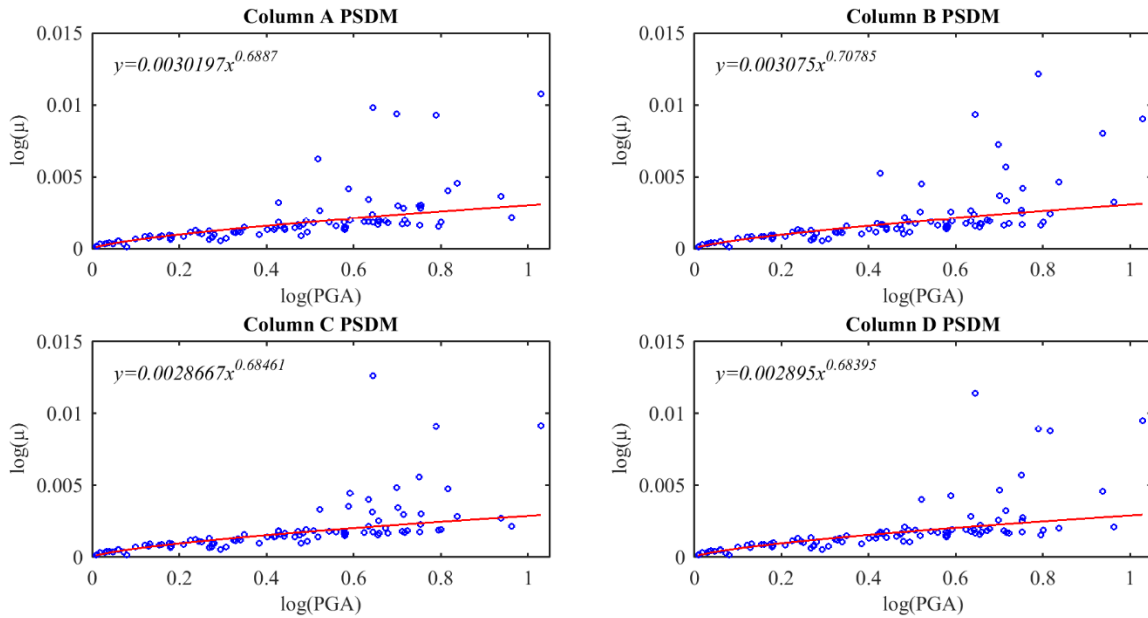


Figure 4.3 Column longitudinal curvatures PSDM for straight bridge

The PSDM results of column-pier shear strength in the longitudinal and transverse directions for the curved and skewed bridge are shown in Figures 4.4 and 4.5, respectively. The column shear PSDM results for the skewed and curved bridge vary among different columns (Figures 4.4-4.5) and the largest one can reach almost twice as that for the straight counterpart.

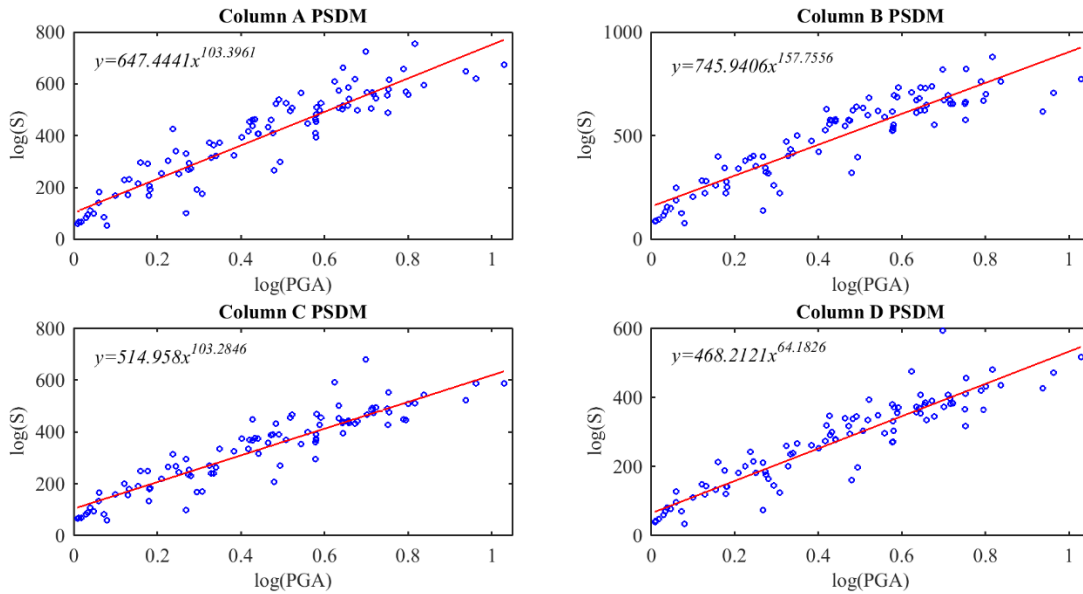


Figure 4.4 PSDM of column longitudinal shear strength for the curved and skewed bridge

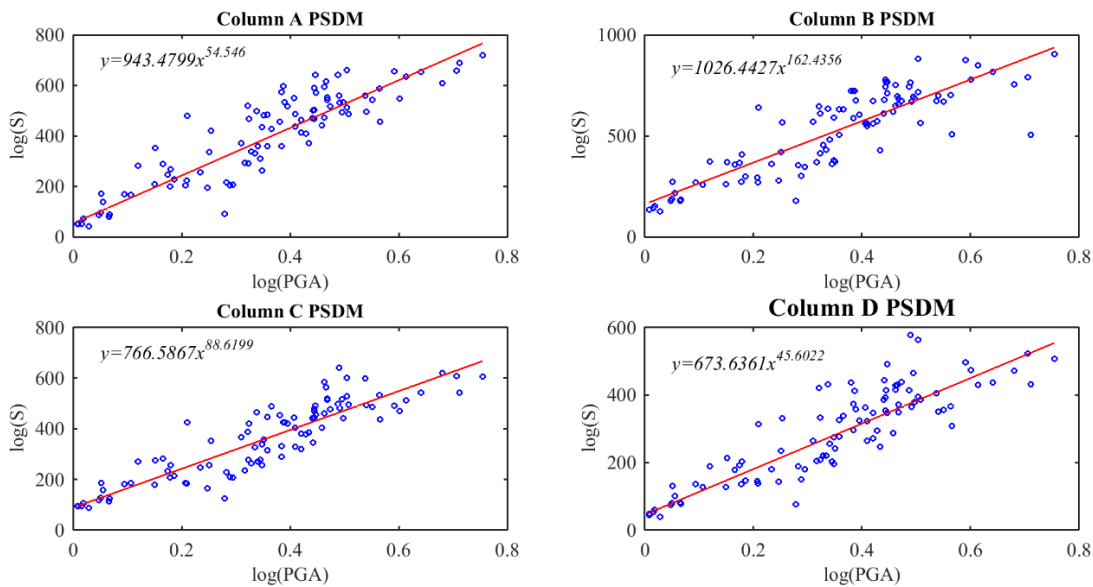


Figure 4.5 PSDM of column transverse shear strength for the curved and skewed bridge
 Note: S=component seismic demand

Figure 4.6 shows regression analysis results of the abutment deformation. The passive and active longitudinal deformations vary only slightly from each other for the skewed and curved bridge. In Figure 4.6, the PSDM comparison shows the wing-wall component would be more fragile when the PGA is over 0.3g. The same phenomenon was found in regression analysis of the skewed-only bridge model, which means curvature may have less influence on the abutment than the skew does. Table 4.2 shows the regression coefficients in Eq. (4.1) and the standard deviation “Beta” and coefficient of determination “ R^2 .”

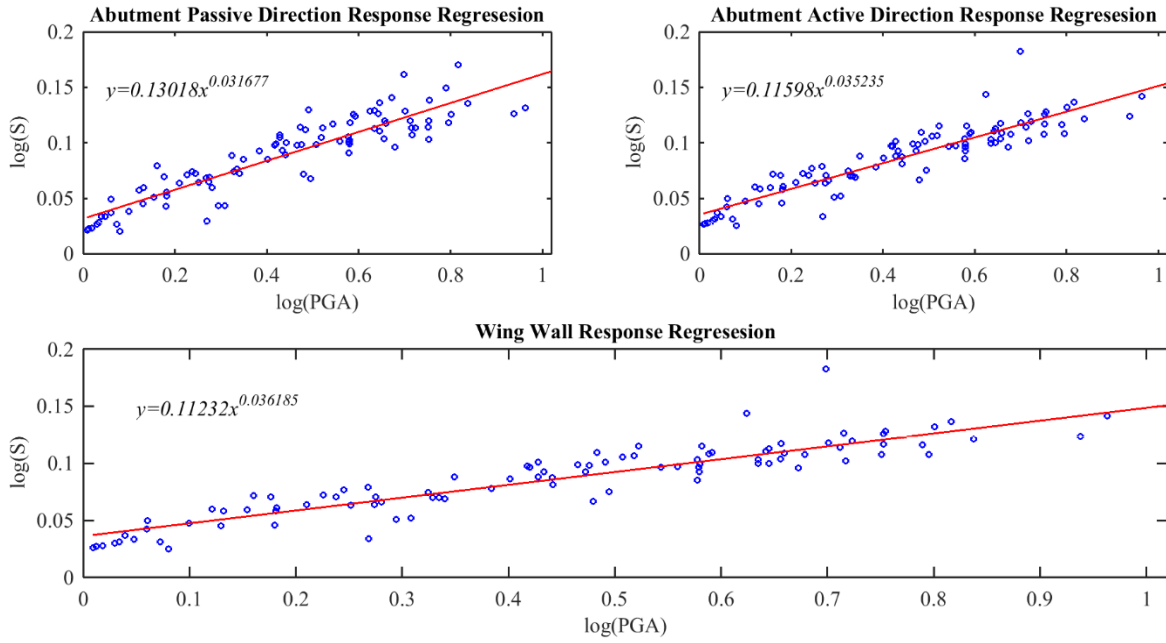


Figure 4.6 PSDM of abutment deformation

Note: Abut-p= abutment passive deformation; Abut-a= abutment active deformation; w= wing-wall deformation

Table 4.2 Probabilistic Seismic Demand Parameter Regression of Straight Bridge Model

Demand Response	a	b	β_d	R^2
Col-Long (A)	0.0037	0.7011	0.928425	0.6977
Col-Long (B)	0.0045	0.882	1.081222	0.8815
Col-Long (C)	0.0024	0.6472	0.802926	0.642
Col-Long (D)	0.0022	0.6368	0.765687	0.6321
Col-Trans(A)	0.0009	0.8242	0.992762	0.7984
Col-Trans(B)	0.0018	0.972	1.239829	0.9671
Col-Trans(C)	0.0006	0.7088	0.883541	0.7028
Col-Trans(D)	0.0004	0.6132	0.73181	0.6249
Shr-Long (A)	658.16	0.5896	0.63103	0.5896
Shr-Long (B)	788.93	0.5475	0.586098	0.5475
Shr-Long (C)	533.3	0.5382	0.578591	0.5382
Shr-Long (D)	452.72	0.5913	0.631935	0.5913
Shr-Trans (A)	802.69	0.6645	0.67295	0.6645
Shr-Trans (B)	880.89	0.4825	0.506952	0.4825
Shr-Trans (C)	606.61	0.4897	0.516396	0.4897
Shr-Trans (D)	552.45	0.6126	0.629689	0.6126
Abut-p (ft)	0.152	0.4892	0.513862	0.4747
Abut-a (ft)	0.1263	0.4419	0.444565	0.4119
Wing (ft)	0.1263	0.4419	0.444586	0.4119

4.4 Fragility Curve

With the PSDM approximated in the previous section and defined limit states from section 4.1, fragility curves were developed following Eq. (4.3). Figures 4.7(a-d) present the component fragility curves for the skewed and curved bridge model, including column flexural curvatures (column A), abutment passive deformation, abutment active deformation and wing wall deformation for different limit states. For the “complete damage” limit state, fragility curves of shear forces in the longitudinal and transverse directions (column A) also are displayed.

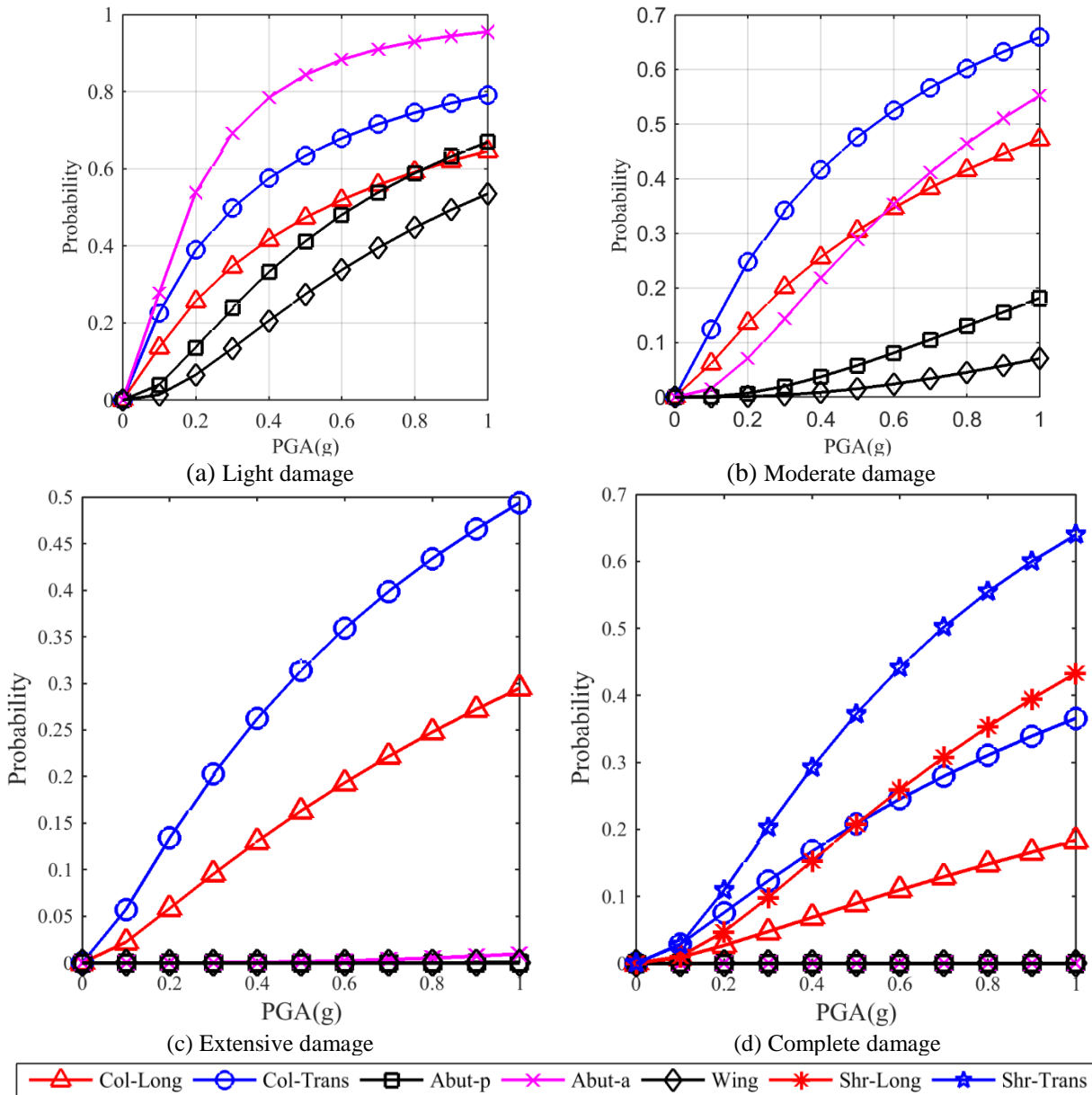


Figure 4.7 Component fragility curves

These fragility curve results suggest that different structural limit states are dominated by seismic performance of different bridge components, respectively. For instance, abutment active deformations tend to have the highest fragility under the light damage limit state. However, when complete damage is concerned, structural failure is governed by column transverse shear. For more critical limit states such as extensive or complete damage, the abutment only has small probability of experiencing excessive deformations. Results also show that columns are more vulnerable to transverse ground motion for almost all the limit states, highlighting the importance of bridge transverse resistance to its serviceability under seismic activity.

4.5 Comparative Study of Critical Factors

In this section, light damage was selected as the baseline for the following column fragilities, due to its sensitivity. Longitudinal curvatures for four individual columns under different geometric configurations are presented in Figures 4.8(a-d). Transverse moment curvature, longitudinal shear and transverse shear fragility curves for individual columns are not shown due to similar trends.

Results show that when compared to the pretty consistent seismic performance among the columns of the straight bridge, skew and curvature cause different fragility levels among different columns. Fragility curves of the four columns of the skewed bridge (Figure 4.8b) tend to marginally “scatter” from each other. This result is consistent with findings made by [Zakeri et al. \(2014\)](#) in their fragility curve study for skewed bridge integral abutments bridge, where fragility curves showed negligible effect from different geometric configurations on the longitudinal moment curvatures.

For fragility curves of the curved bridge model, the out-of-plane rotation of the superstructure results in coupled fragility performance for the columns: fragilities of the two columns in diagonal positions (one interior and one exterior to the superstructure curvature) are similar despite belonging to different piers. By comparing Figures 4.8(b) and (c), it was found that curvature causes more scatterings of fragility performance among columns than skew does. Under the same seismic intensity, it is apparent that curvature causes higher fragility than the skewed or straight bridge counterparts. The curved and skewed bridge exhibits overall the highest fragility among all the configurations under the same seismic intensity. Specifically, the skewed and curved bridge has lower fragility in lower PGA but higher fragility in higher PGA than those of the curved bridge, respectively.

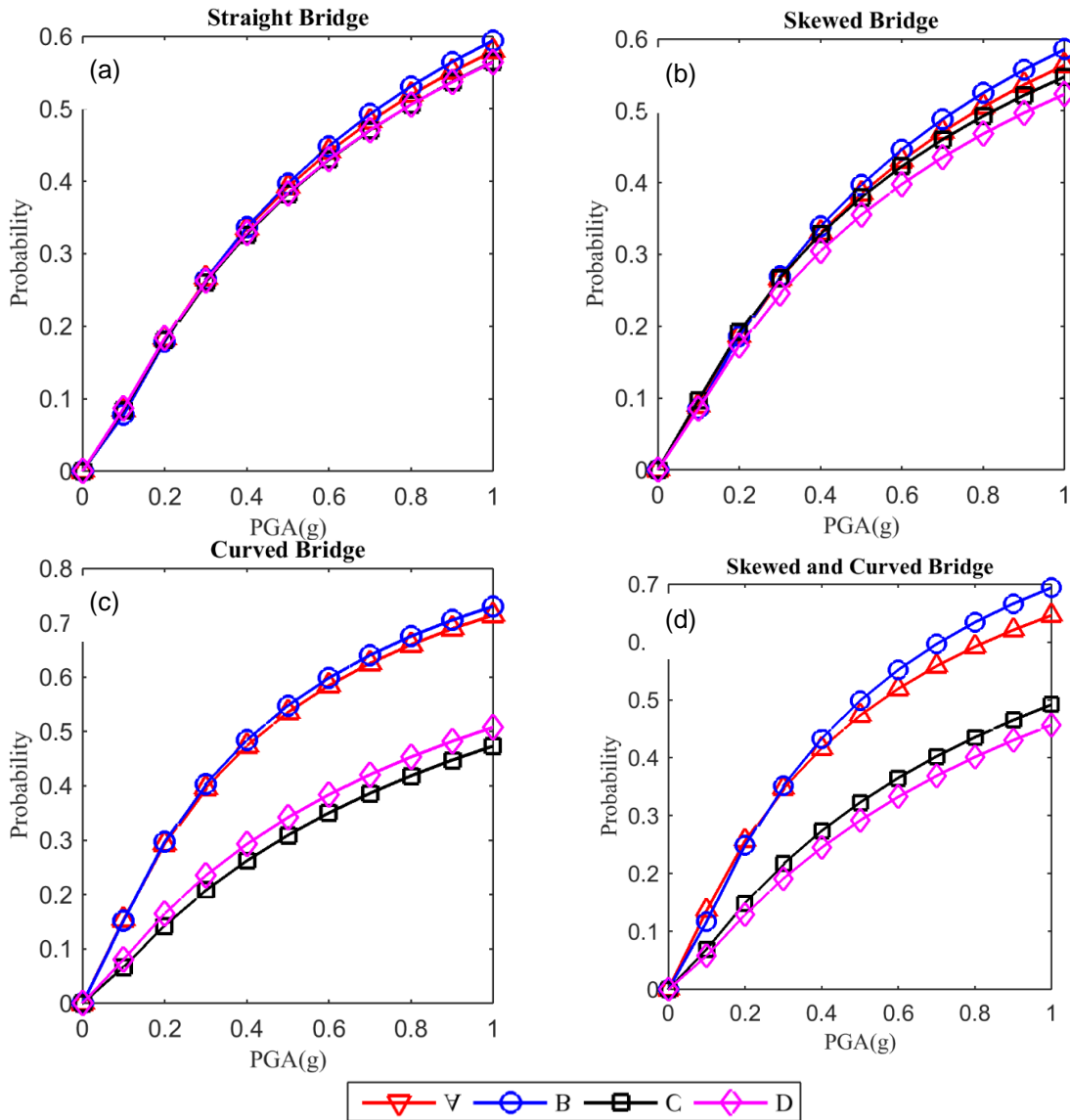


Figure 4.8 Column fragility curves of longitudinal moment curvature under light damage

Figure 4.9 shows the median PGA of each curve with 50% fragility of column curvature under light damage in the longitudinal direction, and median PGA values are inversely proportional to the component fragility. It also shows that for straight and skewed bridges, little difference of medium PGA values exist among four columns. For the curved bridge and both curved and skewed bridges, columns A and B have much lower median PGA than columns C and D. Interestingly, under light damage, the bridge with curvature only has the lowest medium PGA for the column curvature of columns A, B, but not C and D, for which the straight bridge has the lowest medium PGA. It also shows that curvature causes considerable difference between the median PGA values of the interior (A and B) and exterior (C and D) columns, which could reach up to 1.79 times. For the bridge with both curvature and skew, it has lower median PGA for columns A and B, but higher median PGA for columns C and D compared to the straight bridge

baseline model. Such fragility difference suggests the need of conducting designs of individual columns for bridges with curvature.

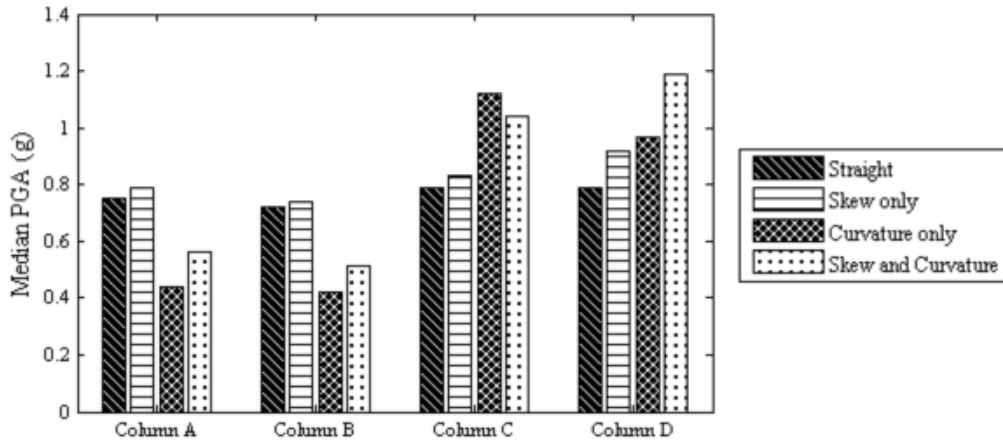


Figure 4.9 Fragility median PGA of column curvature for different models under light damage

In the following section, median PGA values of different limit states are compared with different bridge geometric configurations. Figure 4.10 gives the median PGA results for the moderate damage limit state. Results show that the limit state for “abut-a” (abutment active deformation) has the lowest median PGA among all the limit states and little difference exists among those with different geometric configurations. The second lowest median PGA among all the limit states in Figure 4.10 is that of column transverse moment curvature (“col-trans”), in which bridges with both skew and curvature are the lowest compared to other geometric configurations. For the limit states of “abut-p”, “abut-a” and “wing” limit states (Table 4.2), the both curved and skewed bridge has higher median PGA than the straight bridge and the curved-only bridge.

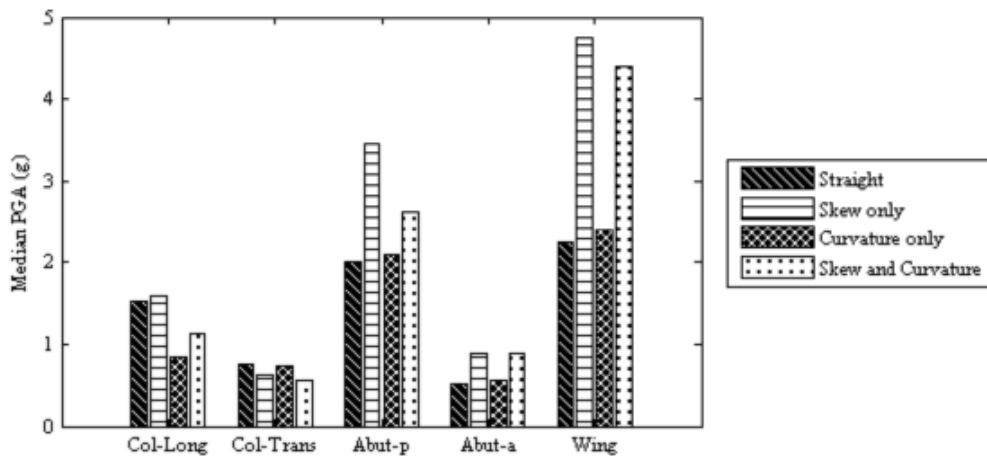


Figure 4.10 Skew and curvature influence on component fragilities under moderate damage state

To illustrate how geometric configuration influences bridge component fragilities, median PGA values of each damage state were compared and shown in Figures 4.11 and 4.12. In Figure 4.11, column seismic fragilities were compared for both transverse and longitudinal directions and it was found that column fragilities of all types of bridge configurations are dominated by transverse response. This is mainly because of the relatively low capacity in the transverse

direction for the columns. Consistent fragility dispersions among different bridge configurations were observed in the longitudinal direction. The difference becomes more significant when the considered damage state increases from light damage to complete damage. Comparison of the results with different geometric configurations suggests that columns of the curved bridges have the lowest median PGA (highest fragility) in the longitudinal direction. This possibly is because the irregular curved superstructure increases the bending moment arm for longitudinal seismic motion, which results in higher curvature, as the major indicator of column fragility. Column transverse fragility, on the other hand, was only slightly affected by such influence.

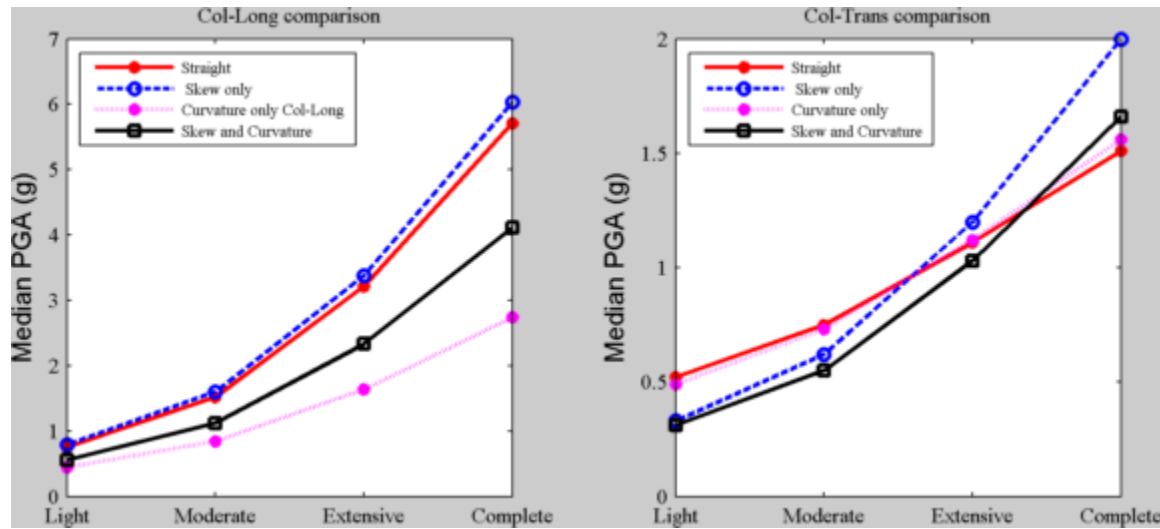


Figure 4.11 Comparison of different geometric configurations under different damage states

The abutment fragility difference between skewed and non-skewed bridge designs also is noteworthy. Figure 4.12 presents the median PGA comparison for abutment fragilities under all damage states for which fragility exceeds 50%. Results from the comparison indicate that the skew nature of the bridge reduces fragilities of the abutment in both passive and active deformations due to compacted soil-structural interaction at the backfill-abutment interface, which supports the common practice of related integral abutment bridge studies.

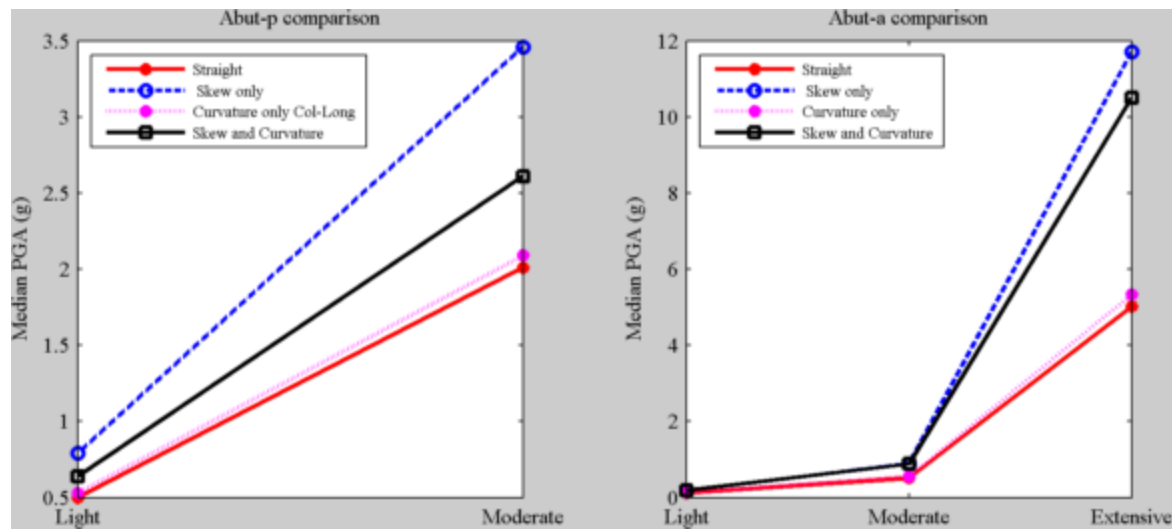


Figure 4.12 Median PGA values comparison for abutment fragilities under different damage states

Figure 4.13 lists the median PGA results of the column shear fragility in both longitudinal and transverse directions for bridges with different geometric configurations. Comparatively, transverse shear of the column generally has the lower median PGA (higher fragility) than that for longitudinal shear regardless of geometric configurations. It was also found that transverse shear is slightly affected by geometric configurations and the straight bridge has the lowest fragility on the transverse shear. Geometric configurations cause, however, much more significant effect on the longitudinal shear, and the curved bridge has the lowest fragility (highest median PGA), followed by the straight bridge. For shear in both directions, the curved and skewed bridge has the highest fragilities (lowest median PGA) among all the geometric configurations and it seems skew plays an important role in affecting shear fragility. Figure 4.12 shows that skew helps to reduce abutment fragility by limiting the abutment longitudinal deformation. Apparently, less deformation also means larger shear forces and increased shear fragilities on the columns.

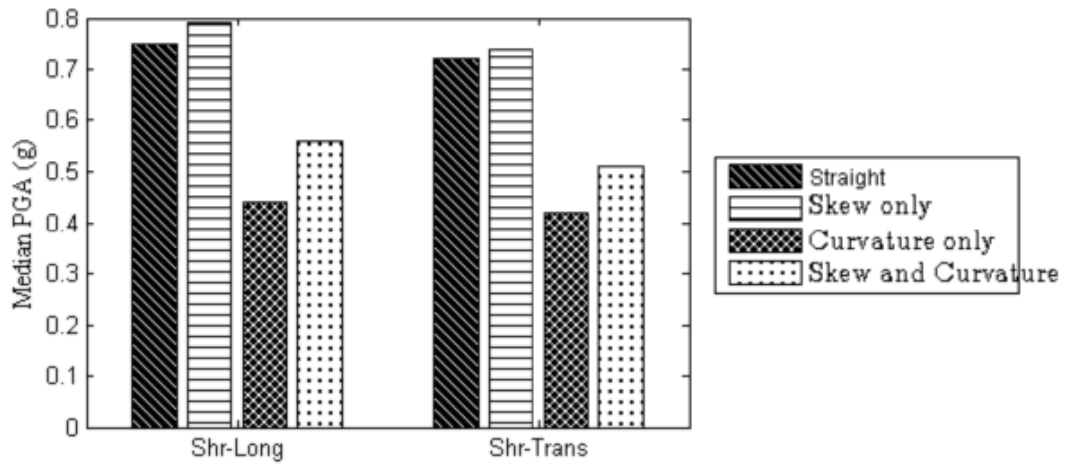


Figure 4.13 Median PGA comparison of skew and curvature influence on shear fragility curves

5. CONCLUSION AND FUTURE WORKS

This study investigated the performance-based seismic assessment of curved and skewed bridges by focusing on fragility analysis results. The influences of skewed and curved geometric configurations on bridge component seismic fragility were investigated by developing analytical fragility curves. A typical 3-span concrete straight bridge located in Denver, CO, was selected as the prototype bridge, from which three bridge models with complex geometric variations were modified. Based on the nonlinear FEM analysis results of these bridge models, fragility analyses were carried out considering the uncertainties of the bridge model and ground motions. Comparative studies also were conducted to investigate influences from the geometric configurations. Some main conclusions are illustrated as following:

1. For the curved and skewed bridge model investigated in this study, it was found that different damage limit states are dominated by the seismic performance of different bridge components. Given the complex seismic risk performance associated with curved and/or skewed configurations, a comprehensive risk assessment of bridges with complex geometric configurations is found important even in low-to-moderate seismic regions;
2. For the skewed and curved bridge, columns were found to have high fragility associated with transverse demands for almost all the limit states, highlighting the importance of the transverse seismic resistance to the serviceability and safety of skewed and curved bridges. Comparatively, bridges with curvature have the highest fragility overall of the longitudinal moment curvature, while the skewed-only bridge has the highest fragility of the transverse moment curvature;
3. As compared to fairly consistent seismic performance among the columns of the straight bridge, skew and curvature nature was found to cause different fragilities on individual columns. Fragility curves for different columns of the skewed bridge are similar and tend to only “scatter” in the high seismic intensity region. For bridges with curvature, fragilities of the interior columns of two intermediate piers are similar, and are considerably higher than the fragility of two exterior columns. The skew nature will cause some difference on fragilities between two interior columns and two exterior columns, respectively. Such fragility difference among columns suggests the need for picking the right column to control the design or conducting column-specific design for individual columns of bridges with curvature.
4. For light damage state, the limit state for “Abut-a” has much lower median PGA overall than other limit states for all bridge models. Bridges with curvature were found to have lower median PGA than other bridges for column longitudinal moment curvature. Bridges with skew have lower median PGA for column transverse moment curvature. For moderate damage state, lowest median PGA was found for the limit state related to column transverse moment curvature.

REFERENCES

- AASHTO (2013). LRFD Bridge Design Specifications, Customary U.S. Units, 6th Edition, with 2013 Interim Revisions
- Billah, A. M., Alam, M. S., and Bhuiyan, M. R. (2012). Fragility Analysis of Retrofitted Multicolumn Bridge Bent Subjected to Near-Fault and Far-Field Ground Motion. *Journal of Bridge Engineering*, 18(10), 992-1004.
- Baker, J. W., and Cornell, C. A. (2005). A vector-valued ground motion intensity measure consisting of spectral acceleration and epsilon. *Earthquake Engineering and Structural Dynamics*, 34(10), 1193-1217.
- Baker, J. W., and Cornell, C. A. (2006). Vector-valued ground motion intensity measures for probabilistic seismic demand analysis. Pacific Earthquake Engineering Research Center, College of Engineering, University of California, Berkeley.
- Berkeley, C. S. I. (2011). Computer program SAP2000 v14. 2.4. Computers and Structures Inc., Berkeley, California.
- Choi, E. (2002). "Seismic analysis and retrofit of Mid-America bridges." Ph.D. thesis, Georgia Institute of Technology, Atlanta.
- California Department of Transportation. (2006). Caltrans Seismic Design Criteria, (1.6), 161.
- Ellingwood, B. and H. Hwang (1985). Probabilistic descriptions of resistance of safetyrelated structures in nuclear plants." *Nuc. Engrg. and Des.* 88(2):169-178.
- Ellingwood, B. R., and Kinali, K. (2009). Quantifying and communicating uncertainty in seismic risk assessment. *Structural Safety*, 31(2), 179-187.
- Fang, J., Li, Q., Jeary, A., and Liu, D. (1999). Damping of Tall Buildings: Its Evaluation and Probabilistic Characteristics. *Structural Design of Tall Buildings*, 8(2), 145–153.
- FEMA (1997) HAZUS. Earthquake loss estimation methodology. Technical Manual, National Institute of Building for the Federal Emergency Management Agency, Washington (DC), 1997
- FEMA (2004) NEHRP Recommended Provisions for Seismic Regulations for New Buildings and Other Structures, 2003 Edition, Part 1 – Provisions, Part 2 – Commentary. FEMA 450. Federal Emergency Management Agency. Washington, DC.
- Kowalsky, M. J., and Priestley, M. N. (2000). Improved analytical model for shear strength of circular reinforced concrete columns in seismic regions. *ACI Structural Journal*, 97(3).
- Kwon, O. S., and Elnashai, A. S. (2007). Fragility Analysis of a Bridge with Consideration of Soil-Structure-Interaction Using Multi-Platform Analysis. In *Structural Engineering Research Frontiers* (pp. 1-14). ASCE.
- MacGregor, J. G., Wight, J. K., Teng, S., & Irawan, P. (1997). Reinforced concrete: mechanics and design (Vol. 3). Upper Saddle River, NJ: Prentice Hall.
- Mackie, K. R., and Stojadinović, B. (2007). Performance-based seismic bridge design for damage and loss limit states. *Earthquake Engineering and Structural Dynamics*, 36(13), 1953-1971.
- Matthews, V. (2003). The challenges of evaluating earthquake hazard in Colorado. *Engineering Geology in Colorado: Contributions, Trends, and Case Histories*.
- Maragakis, E. (1984). A model for the rigid body motions of skew bridges.

- Mwafy, A. M., and Elnashai, A. S. (2007). Assessment of seismic integrity of multi-span curved bridges in mid-America.
- Neves, L. A., Frangopol, D. M., and Cruz, P. J. (2006). Probabilistic lifetime-oriented multiobjective optimization of bridge maintenance: Single maintenance type. *Journal of Structural Engineering*, 132(6), 991-1005.
- Nielson, B. G. (2005). Analytical fragility curves for highway bridges in moderate seismic zones, Ph.D. dissertation, Georgia Institute of Technology.
- Nielson, B. G., and DesRoches, R. (2007). Seismic fragility methodology for highway bridges using a component level approach. *Earthquake Engineering and Structural Dynamics*, 36(6), 823-839.
- Pan, Y., Agrawal, A. K., and Ghosn, M. (2007). Seismic fragility of continuous steel highway bridges in New York State. *Journal of Bridge Engineering*, 12(6), 689-699.
- Padgett, J. E., and DesRoches, R. (2007). Sensitivity of seismic response and fragility to parameter uncertainty. *Journal of Structural Engineering*, 133(12), 1710-1718.
- Padgett, J. E., and DesRoches, R. (2008). Methodology for the development of analytical fragility curves for retrofitted bridges. *Earthquake Engineering and Structural Dynamics*, 37(8), 1157-1174.
- Priestley, M. J. N., Seible, F. and Calvi, G. M. (1996), *Seismic Design and Retrofit of Bridges*, John Wiley & Sons, New York, USA
- Rix, G. J., and Fernandez-Leon, J. A. (2004). Synthetic ground motions for Memphis, TN. [http://www.ce.gatech.edu/research/mae_ground_ motionæ](http://www.ce.gatech.edu/research/mae_ground_motionæ) (Jul. 5, 2008).
- Sullivan, I., and Nielson, B. G. (2010, May). Sensitivity analysis of seismic fragility curves for skewed multi-span simply supported steel girder bridges. In *Proceedings of 19th Analysis and Computation Specialty Conference, Structures Congress* (pp. 226-237).
- Saiidi, M., and Orié, D. (1992). Earthquake design forces in regular highway bridges. *Computers and structures*, 44(5), 1047-1054.
- Shinozuka, M., Kim, S. H., Kushiyama, S., and Yi, J. H. (2002). Fragility curves of concrete bridges retrofitted by column jacketing. *Earthquake Engineering and Engineering Vibration*, 1(2), 195-205.
- Sucuoğlu, H., and Erberik, A. (2004). Energy-based hysteresis and damage models for deteriorating systems. *Earthquake engineering and structural dynamics*, 33(1), 69-88.
- Vickery, P. J., Skerlj, P. F., Lin, J., Twisdale Jr, L. A., Young, M. A., and Lavelle, F. M. (2006). HAZUS-MH hurricane model methodology. II: Damage and loss estimation. *Natural Hazards Review*, 7(2), 94-103.
- WSDOT (2002). Design Manual, Program Development Division, Washington State Department of Transportation, Olympia, WA. (<http://www.wsdot.wa.gov/Publications/Manuals/M22-01.htm>)
- Wen, Y. K., and Wu, C. L. (2001). Uniform hazard ground motions for Mid-America cities. *Earthquake spectra*, 17(2), 359-384.
- Wilson, T., Mahmoud, H., and Chen, S. (2014). Seismic performance of skewed and curved reinforced concrete bridges in mountainous states. *Engineering Structures*, 70, 158-167.
- Xiao, Y., and Ma, R. (1997). Seismic retrofit of RC circular columns using prefabricated composite jacketing. *Journal of Structural Engineering*, 123(10), 1357-1364.
- Zhang, J., and Huo, Y. (2009). Evaluating effectiveness and optimum design of isolation devices for highway bridges using the fragility function method. *Engineering Structures*, 31(8), 1648-1660.

Zakeri, B., Padgett, J. E., and Amiri, G. G. (2014). Fragility analysis of skewed single frame concrete box girder bridges. *Journal of Performance of Constructed Facilities*, 28(3), 571–582.